

FAST CONTROL OF QUANTUM STATES IN QUANTUM DOTS: LIMITS DUE TO DECOHERENCE

Lucjan Jacak, Paweł Machnikowski

Institute of Physics, Wrocław University of Technology, 50-370 Wrocław, Poland

Jurij Krasnyj

*Institute of Mathematics, University of Opole, 45-051 Opole, Poland**

Abstract We study the kinetics of confined carrier-phonon system in a quantum dot under fast optical driving and discuss the resulting limitations to fast coherent control over the quantum state in such systems.

1. Introduction

Unlike natural atoms, semiconductor quantum dots (QDs) always form part of a macroscopic crystal. The interaction with the quasi-continuum of lattice degrees of freedom (phonons) constitutes an inherent feature of these nanometer-size systems and cannot be neglected in any realistic modeling of QD properties, especially when the coherence of confined carriers is of importance. The understanding of the decisive role played by the QD coupling to lattice modes has increased recently due to both experimental and theoretical study (spectrum reconstruction [1–4], relaxation [5–10], phonon replicas and phonon-assisted transitions [11–16], phonon-induced pure dephasing upon ultrafast excitation [17–22]). The phonon-induced decoherence seems to be crucial for any quantum information processing application and for any nanotechnological device relying on quantum coherence of confined carriers [23, 24].

There are three major mechanisms of carrier-phonon interaction [25]: (1) Coulomb interaction with the lattice polarization induced by the relative shift of the positive and negative sub-lattices of the polar compound,

*On leave from Odessa University, Ukraine

described upon quantization by longitudinal optical (LO) phonons; (2) deformation potential coupling describing the band shifts due to lattice compression, i.e. longitudinal acoustical (LA) phonons; (3) Coulomb interaction with piezoelectric field generated by shear crystal deformation (transversal acoustical, TA, phonons). The lattermost effect is weak in InAs/GaAs systems but may be of more importance for the properties e.g. of GaN dots [26–28].

Due to the carrier-phonon interaction, any change in the carrier subsystem must be accompanied by the appropriate modification of the lattice state. An example of this effect may be creation of the exciton-polaron states: excitons accompanied by the lattice polarization (coherent LO phonon field) with energy shifted down by a few meV [3, 22]. The interaction with acoustical branches leads to creation of a similar deformation field which, although much less pronounced in terms of energy shift, strongly influence the dynamical properties of the interacting system due to gapless spectrum and low characteristic frequencies of the acoustical phonons.

The lattice response to any manipulation performed on the charge distribution confined in a QD leads to discrepancy between the desired state of the quantum confined system and the actual one. This effect may be stronger than any decoherence process in an undriven system. In terms of the quantum information processing schemes, such a discrepancy is manifested by the loss of fidelity of the quantum operation. In quantum nano-technology applications, it will reduce the efficiency of nano-devices.

In the present paper we discuss the carrier-lattice kinetics induced by optical excitation of a confined exciton. The paper is organized as follows: In the next section we present the formal model of the exciton confined in a QD. The section 1.3 describes the system kinetics in response to an abrupt change of the charge distribution. In the section 1.4 we discuss the trade-off between the dynamically induced error and other processes limiting the coherence time of a quantum state. The final section contains concluding discussion.

2. The model

We consider the Hamiltonian describing a single exciton interacting with phonons,

$$\begin{aligned}
 H = & \sum_n \epsilon_n a_n^\dagger a_n + \sum_{\mathbf{k}, s} \omega_{s, \mathbf{k}} b_{s, \mathbf{k}}^\dagger b_{s, \mathbf{k}} \\
 & + \frac{1}{\sqrt{N}} \sum_{\mathbf{k}, n, n', s} F_{n, n'}^{(s)}(\mathbf{k}) a_n^\dagger a_{n'} \left(b_{s, \mathbf{k}} + b_{s, -\mathbf{k}}^\dagger \right),
 \end{aligned}$$

Electron mass	m_e	$0.067m_0$
Hole mass	m_h	$0.38m_0$
Static dielectric constant	ε_s	13.2
Effective dielectric constant	$\tilde{\varepsilon}$	62.6
Optical phonon energy	Ω_0	36 meV
Longitudinal sound speed	c	5150 m/s
Deformation potential for electrons	σ_e	6.7 eV
Deformation potential for holes	σ_h	-2.7 eV
Unit crystal cell volume	v	0.044 nm^3
LO phonon dispersion parameter	β	$0.03 \text{ meV}\cdot\text{nm}^2$

Table 1. The material parameters used in the calculations (partly after Refs. [29, 30]).

where $b_{s,\mathbf{k}}, b_{s,\mathbf{k}}^\dagger$ are bosonic annihilation and creation operators for LO ($s = o$) and LA ($s = a$) phonons with quasi-momentum \mathbf{k} . The corresponding frequencies within the effectively coupled wavevector range may be modeled by $\omega_{o,\mathbf{k}} = \Omega_{\mathbf{k}} \simeq \Omega - \beta k^2$ and $\omega_{a,\mathbf{k}} = ck$. The coupling constants for the LO and LA phonon branches are given by

$$F_{n,n'}^{(o)}(\mathbf{k}) = -\frac{e}{k} \sqrt{\frac{2\pi\Omega}{v\tilde{\varepsilon}}} \int \Phi_n^*(\mathbf{r}_e, \mathbf{r}_h) \left(e^{i\mathbf{k}\cdot\mathbf{r}_e} - e^{i\mathbf{k}\cdot\mathbf{r}_h} \right) \Phi_{n'}(\mathbf{r}_e, \mathbf{r}_h) d^3\mathbf{r}_e d^3\mathbf{r}_h$$

and

$$F_{n,n'}^{(a)}(\mathbf{k}) = -\sqrt{\frac{k}{2\rho vc}} \int \Phi_n^*(\mathbf{r}_e, \mathbf{r}_h) \left(\sigma_e e^{i\mathbf{k}\cdot\mathbf{r}_e} - \sigma_h e^{i\mathbf{k}\cdot\mathbf{r}_h} \right) \Phi_{n'}(\mathbf{r}_e, \mathbf{r}_h) d^3\mathbf{r}_e d^3\mathbf{r}_h, \quad (1)$$

where $\mathbf{r}_e, \mathbf{r}_h$ denote the coordinates of the electron and hole, respectively, and $\Phi_n(\mathbf{r}_e, \mathbf{r}_h)$ is the exciton wavefunction. The other elements of the notation are described in Table 1, along with values (corresponding to InAs/GaAs system) used in the calculations.

Numerical diagonalization of the interacting electron-hole system in parabolic confinement, under assumption that non-interacting electron and hole would have the same wavefunctions, leads to the spectrum shown in Fig. 1a (M is the conserved total angular momentum). The dominant contribution to the lowest excited states of the exciton comes from the excited hole states, while the electron wavefunction is only slightly modified. The corresponding electron and hole distributions are shown in Fig. 1b-d.

The exciton-phonon coupling functions may be calculated using the wavefunctions found numerically. Fig. 2 (left panels) shows the results

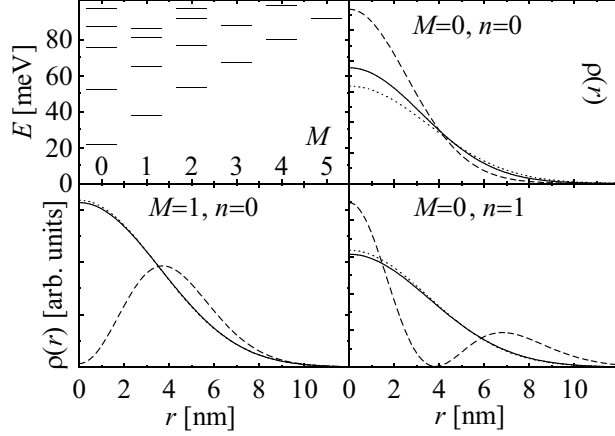


Figure 1. The spectrum of the exciton in QD (upper left) and the electron (solid lines) and hole (dashed lines) probability densities for the three lowest exciton states, compared to the ground state probability density for a noninteracting particle (dotted lines). Here the noninteracting particle wavefunction width is $l_{\perp} = 4.9$ nm in-plane and $l_z = 2$ nm in the growth direction.

for coupling between the ground state and a few lowest states, averaged over angles. The coupling to LO phonons is much stronger than to LA phonons. In the case of LO phonons, the coupling strength increases for excited states due to less charge cancellation between the electron and hole in these states (cf. Fig. 1b-d).

3. System kinetics after an ultrafast pulse

Let us study the kinetics of the system after an excitation performed by an extremely short (formally infinitely short) laser pulse. The information on the dynamics of the interacting carrier-lattice system is contained in the exciton single-particle causal Green function,

$$G_{n,n'}(t) = -i\langle T\{a_n(t)a_{n'}^{\dagger}(0)\}\rangle.$$

The averaging $\langle \dots \rangle$ is the temperature-dependent averaging with respect to phonon degrees of freedom and the vacuum of exciton (cf. Ref. [31]; it corresponds to the case when the grand canonical averaging sector without exciton, vacuum, is energetically distant, ~ 1 eV, from the next sectors). For $t \geq 0$ this Green function coincides (up to a constant factor) with the correlation function $\langle a_n(t)a_{n'}^{\dagger}(0) \rangle$ which, for $n_1 = n_2$ may be interpreted as a measure of integrity of the excitonic state: it corresponds to the overlap of the state at time t with this state at the

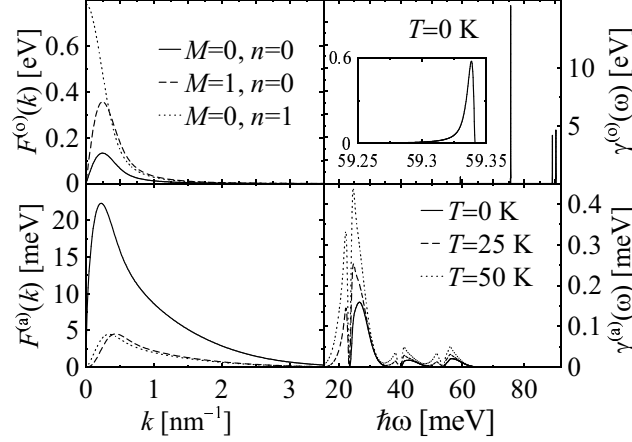


Figure 2. Coupling constants for LA (a) and LO (b) phonon modes between the ground state and the three lowest states and the resulting structure of the imaginary part of the mass operator (c,d).

initial moment $t = 0$. The Fourier transform of the correlation function, $I_{n,n'}(\omega) = \int_{-\infty}^{\infty} \langle a_n(t) a_{n'}^\dagger(0) \rangle e^{i\omega t} dt$, is usually called the spectral density [32, 33], and it can be expressed by the imaginary part of the causal Green function:

$$\text{Im} G_{n,n'}(\omega) = -\frac{1}{2} \left(1 + e^{-\omega/k_B T} \right)^{-1} I_{n,n'}(\omega), \quad (2)$$

where $G_{n,n'}(\omega) = \int_{-\infty}^{\infty} G_{n,n'}(t) e^{i\omega t} dt$.

The equation of motion for the causal Green function may be rewritten as a Dyson-type equation,

$$(\omega - \epsilon_n) G_{n,n'}(\omega) - \sum_{n_3} M_{n,n''}(\omega) G_{n'',n'}(\omega) = \delta_{n,n'}, \quad (3)$$

with the mass operator

$$M_{n,n'}(\omega) = \frac{i}{2\pi N} \sum_{\mathbf{k}, s, n'', n'''} F_{n,n''}^{(s)}(\mathbf{k}) F_{n''',n'}^{(s)}(-\mathbf{k}) \times \int d\omega' G_{n'',n'''}(\omega + \omega') D^0(\mathbf{k}, s, \omega'),$$

where we have restricted ourselves to single-phonon processes by replacing the vertex function by its zeroth order approximation and using the free phonon Green function (LO phonon damping may be easily included later: see below). Since $F_{n,n'}^{(s)}(\mathbf{k}) \sim g_s$, then $|M_{n,n'}(\omega)|^2 \sim g_s^2$. Hence, up

to g_s^2 one has from Eq. (3),

$$G_{n,n}(\omega) = \frac{1}{\omega - \epsilon_n - M_{n,n}(\omega)} \quad (4)$$

and

$$\begin{aligned} M_{nn}(\omega) &= \Delta_n(\omega) - i\gamma(\omega) \\ &= \frac{i}{2\pi N} \sum_{n', \mathbf{k}} |F_{nn'}^{(s)}(\mathbf{k})|^2 \int d\omega' G_{n'n'}(\omega + \omega') D^{(0)}(s, \mathbf{k}, \omega'). \end{aligned} \quad (5)$$

For the real and the imaginary part of the mass operator we obtain form (5)

$$\begin{aligned} \Delta_n(\omega) &= \frac{1}{N} \sum_{\mathbf{k}, s, n,} |F_{nn'}^{(s)}(\mathbf{k})|^2 \\ &\times \left[\frac{(1 + n_{s,\mathbf{k}})(\omega - \epsilon_{n'} - \Delta_{n'}(\omega - \omega_{s,\mathbf{k}}) - \omega_{s,\mathbf{k}})}{[\omega - \epsilon_{n'} - \Delta_{n'}(\omega - \omega_{s,\mathbf{k}}) - \omega_{s,\mathbf{k}}]^2 + \gamma_{n'}^2(\omega - \omega_{s,\mathbf{k}})} \right. \\ &\left. + \frac{n_{s,\mathbf{k}}(\omega - \epsilon_{n'} - \Delta_{n'}(\omega + \omega_{s,\mathbf{k}}) + \omega_{s,\mathbf{k}})}{[\omega - \epsilon_{n'} - \Delta_{n'}(\omega + \omega_{s,\mathbf{k}}) + \omega_{s,\mathbf{k}}]^2 + \gamma_{n'}^2(\omega + \omega_{s,\mathbf{k}})} \right] \end{aligned} \quad (6)$$

and

$$\begin{aligned} \gamma_n(\omega) &= \frac{1}{N} \sum_{\mathbf{k}, s, n'} |F_{nn'}^{(s)}(\mathbf{k})|^2 \\ &\times \left[\frac{(1 + n_{s,\mathbf{k}})\gamma_{n'}(\omega - \omega_{s,\mathbf{k}})}{[\omega - \epsilon_{n'} - \Delta_{n'}(\omega - \omega_{s,\mathbf{k}}) - \omega_{s,\mathbf{k}}]^2 + \gamma_{n'}^2(\omega - \omega_{s,\mathbf{k}})} \right. \\ &\left. + \frac{n_{s,\mathbf{k}}\gamma_{n'}(\omega + \omega_{s,\mathbf{k}})}{[\omega - \epsilon_{n'} - \Delta_{n'}(\omega + \omega_{s,\mathbf{k}}) + \omega_{s,\mathbf{k}}]^2 + \gamma_{n'}^2(\omega + \omega_{s,\mathbf{k}})} \right]. \end{aligned} \quad (7)$$

In this equation the first term determines the energy shift due to dressing with LO phonons, while the second one corresponds to LA phonons. The former dominates energetically: the energy shift is mainly due to the interaction of exciton with optical phonons (dressing of exciton with LO phonons, creating together an exciton-polaron). The latter is small and its energetical effect may be safely neglected but it contributes considerably to the system kinetics.

To the lowest order, one may neglect $\Delta_{n'}$ and $\gamma_{n'}$ in the right-hand-side of (6) and, neglecting the acoustic phonon term, write the equation for the exciton-polaron energy levels E_n as the poles of the Green function (4), $E_n - \epsilon_n - \Delta_n(E_n) = 0$, i.e.

$$E_n - \epsilon_n - \frac{1}{N} \sum_{\mathbf{k}, n} |F_{nn}^{(o)}(\mathbf{k})|^2 \left[\frac{1 + n_{o,\mathbf{k}}}{E_n - \epsilon_n - \Omega} + \frac{n_{o,\mathbf{k}}}{E_n - \epsilon_n + \Omega} \right] = 0. \quad (8)$$

At $k_B T \ll \Omega$, the above equation is equivalent to that found by Davydov diagonalization of the Fröhlich Hamiltonian for exciton [34]. The Eq. (8) for $n = 0$ gives the ground state energy shift $\Delta_0 \sim -5$ meV for the QD with parameters listed in Table 1 (see Ref. [22]).

The imaginary part of the mass operator is given to the leading order by the equation (putting $\gamma_{n'} = 0$ in the rhs. of Eq. (7)):

$$\begin{aligned} \gamma_n(\omega) = & \quad (9) \\ & \frac{\pi}{N} \sum_{\mathbf{k}, n} \left\{ |F_{nn'}^{(o)}(\mathbf{k})|^2 [(1 + n_{o,\mathbf{k}})\delta(\omega - E_{n'} - \Omega_{\mathbf{k}}) + n_{o,\mathbf{k}}\delta(\omega - E_{n'} + \Omega_{\mathbf{k}})] \right. \\ & \left. + |F_{nn'}^{(a)}(\mathbf{k})|^2 [(1 + n_{a,\mathbf{k}})\delta(\omega - E_{n'} - ck) + n_{a,\mathbf{k}}\delta(\omega - E_{n'} + ck)] \right\}, \end{aligned}$$

where we use the fact that the equation $\omega - \epsilon_{n'} - \Delta_{n'}(\omega \pm \omega_{s,\mathbf{k}}) \pm \omega_{s,\mathbf{k}} = 0$ is solved by $\omega = E_{n'} \mp \omega_{s,\mathbf{k}}$ and neglected higher-order corrections resulting from resolving the Dirac δ . The first term in Eq. (9) describes the energy transfer to the LO phonon sea, while the second one corresponds to the energy transfer from gradually dressing exciton to the LA phonon sea.

The form of $\gamma_0(\omega)$ for our model, including a few lowest states, obtained using the numerical wavefunctions is shown for various temperatures in Fig 2c,d.

Using (4), one finds

$$\text{Im}G_{n,n}(\omega) = \frac{\gamma_n(\omega)}{[\omega - \epsilon_n - \Delta_n(\omega)]^2 + \gamma_n^2(\omega)}. \quad (10)$$

In the following, we will focus on the ground exciton state, $n = 0$. Usually, this state is long-living at low temperatures: the broadening of the corresponding spectral line, related to radiative lifetime and thermally activated processes, does not exceed 0.1 meV for $T < 100$ K [35, 17].

Let us note that the term $\gamma_0^2(\omega)$ in the denominator of (10) is important only near E_0 , where the other term vanishes (otherwise, it is a higher-order correction). Therefore, it may be approximated by a constant $\gamma_0 = \gamma_0(E_0)$. In a similar manner, the correction $\Delta_0(\omega)$ may be replaced by $\Delta_0(\omega) \approx \Delta_0(E_0) + (\omega - E_0)(d\Delta_0(\omega)/d\omega)_{\omega=E_0}$ and combined with ϵ_0 to give E_0 , in accordance with (8).

Thus, one may write for $I_0(\omega) = -(1/\pi)\text{Im}G_{00}(\omega)$

$$\begin{aligned} I_0(\omega) = & \quad (11) \\ & Z^{-1} \frac{1}{\pi} \frac{\gamma_0/2}{(\omega - E_0)^2 + \gamma_0^2/4} \\ & + \sum_{n,s,\mathbf{k}} |F_{0n}^{(s)}(\mathbf{k})|^2 \frac{(n_{s,\mathbf{k}} + 1)\delta(\omega - E_n - \omega_{s,\mathbf{k}}) + n_{s,\mathbf{k}}\delta(\omega - E_n + \omega_{s,\mathbf{k}})}{(\omega - E_0)^2 + \gamma_0^2}, \end{aligned}$$

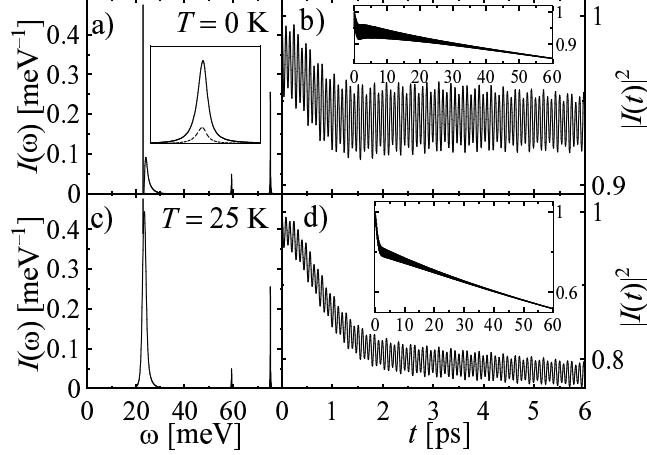


Figure 3. Left: Spectral density vs energy (inset shows the shape of the LO phonon replica) Right: The corresponding evolution of the correlation function for two temperatures, as shown (Insets show the evolution on longer timescales). The calculation is limited to the two lowest exciton states.

where

$$Z = 1 - \frac{d\Delta(\omega)}{d\omega}\bigg|_{\omega=E_0} \approx 1 + \frac{1}{N} \sum_{\mathbf{k},s,n'} \left| \frac{F_{nn'}^{(s)}(\mathbf{k})}{E_{n'} - E_n + \omega_{s,\mathbf{k}}} \right|^2 [1 + 2n_{s,\mathbf{k}}].$$

The Fig. 3a,c shows the result.

At $T = 0$, $\gamma_0(\omega) = 0$ at $\omega = E_0$ (neglecting recombination process) and this point is a well defined pole of the causal Green function. It corresponds to a quasiparticle: the dressed exciton (i.e. the exciton-polaron, if neglecting LA phonons). For $T > 0$, this spectral density has a Lorentzian shape around $\omega \sim E_0$, with width γ_0 . Our model is unable to quantitatively account for the broadening found in experiment. In fact, to our knowledge, its origin has not been explained so far; we will use the experimental values of γ_0 corresponding to 630 ps and 170 ps exciton lifetime (including radiative porocesses and thermally induced transitions) at $T = 0$ K and $T = 25$ K, respectively [17].

Apart from the central peak, the spectral density shows acoustic and optical phonon sidebands. To the former, only the ground state itself contributes: the magnitude of the features visible in $\gamma(\omega)$ around excited states (Fig. 2c,d) is much smaller than the energy distance between these states. Therefore, as far as the interaction with acoustical phonons is concerned, a single level (independent boson) model supplemented by central line broadening is very accurate.

The features resulting from the LO phonon branch behave in a different manner: the contribution from nonadiabatic coupling to excited states is considerable. This results from the fact that the coupling to LO phonons is much stronger in general, the energies of LO phonons are comparable to the exciton energy spacing and the coupling to excited levels is stronger than to the ground state itself due to partial charge cancellation in the latter. In this case, the contribution from the higher states dominates over the ground state contribution and the independent boson approach is not valid.

The time evolution of the dressing process is described by the inverse Fourier transform of the correlation function given by (2). Taking into account that for ω in the energy sector of exciton (of order of eV) $\omega \gg k_B T$, one has

$$I_n(t) = -\frac{1}{\pi} \int_{-\infty}^{\infty} d\omega \text{Im} G_{n,n}(\omega) e^{-i\omega t}.$$

The time-dependent correlation function may be obtained from (11),

$$I_0(t) = Z^{-1} e^{-i(E_0 - i\gamma_0/2)t} + \frac{1}{N} \sum_{n,s,\mathbf{k}} |F_{0n}^{(s)}(\mathbf{k})|^2 \left[\frac{(n_{\mathbf{k}} + 1) e^{-i(E_n + \omega_{s,\mathbf{k}})t}}{(\Delta E_{n0} + \omega_{s,\mathbf{k}})^2 + \gamma_0^2} + \frac{n_{\mathbf{k}} e^{-i(E_n - \omega_{s,\mathbf{k}})t}}{(\Delta E_{n0} - \omega_{s,\mathbf{k}})^2 + \gamma_0^2} \right],$$

where $\Delta E_{n0} = E_n - E_0$. The result, calculated numerically for various temperatures, is plotted in Fig. 3b,d.

The smooth sidebands of $I(\omega)$ correspond to the initial correlation decay on 1 ps timescale. The LO phonon peaks lead to slowly decaying fast oscillations manifesting phonon beats with frequencies corresponding to the energy differences $E_n - E_0 - \Omega$. Without including anharmonic effects, these oscillations would decay very slowly due to the weak LO phonon dispersion. When the anharmonic phonon damping (corresponding to $\tau_{\text{LO}} = 9$ ps decay of an LO phonon [36, 37]) is included by substituting $\omega_{o,\mathbf{k}} \rightarrow \omega_{o,\mathbf{k}} \pm i\gamma_{\text{LO}}$, the LO phonon beats decay with characteristic time slightly below τ_{LO} , which results from the joint effect of damping and dispersion. The long-time dynamics is governed by the Lorentzian feature around $\omega = E_0$ and shows an exponential decay (as assumed beforehand).

4. System response for finite-duration pulses

In the previous section we have shown that any change in the carrier distribution in a QD is followed by lattice relaxation (dressing) processes which lead to some loss of the quantum coherence. To preserve the coherence while operating on the carrier states, the action must be adiabatic

with respect to lattice timescales, i.e. phonon periods. Slowing down the dynamics leads, however, to increasing effect of other decoherence mechanisms, like radiative recombination or thermally activated transitions to higher states, as the decoherence caused by such effects increases linearly with time.

In order to study the interplay of these decoherence effects we have studied the evolution of an exciton coupled to acoustic phonons under optical excitation by a finite-duration laser pulse [23]. The effect of coupling to phonons was quantified in terms of the error of a coherent operation, $\delta = 1 - F$, where the fidelity is defined as an overlap between the actual state and the desired one (the latter was taken to be the dressed final state, obtained by adiabatic operation), $F = \langle \phi | \rho | \phi \rangle$, where $|\phi\rangle$ is the ideal final state and ρ is the final density matrix.

The density matrix for the final state is calculated using second order expansion for the evolution operator of the total system and tracing over the lattice degrees of freedom (see [23, 38] for details). For timescales relevant here, it is sufficient to consider acoustic phonons and only one (ground) exciton state. The error averaged over initial states can be represented as the overlap of two functions

$$\delta = \int \frac{d\omega}{\omega^2} R(\omega) S(\omega),$$

where $R(\omega)$ is the spectral density of the reservoir

$$R(\omega) = \sum_{\mathbf{k}} [\delta(\omega_{\mathbf{k}} - \omega)(n_{\mathbf{k}} + 1) + \delta(\omega_{\mathbf{k}} + \omega)n_{\mathbf{k}}] |F(\mathbf{k})|^2.$$

The function $S(\omega)$ represents spectral characteristics of the system and is given by

$$S(\omega) = \frac{1}{3}(|F_-(\omega)|^2 + |F_+(\omega)|^2), \quad |F_{\pm}(\omega)|^2 \approx \alpha^2 e^{-\frac{1}{2}\tau_g^2 \left(\omega \pm \frac{\alpha}{\sqrt{2\pi}\tau_g}\right)^2}, \quad (12)$$

for a Gaussian driving pulse $f(t) = \alpha/(\sqrt{2\pi}\tau_g)e^{-\frac{1}{2}(t/\tau_g)^2}$, rotating the state by the angle α on the Bloch sphere.

For the coupling (1) to LA phonons, one finds at $T = 0$ for $\omega \ll cl_{\perp}^{-1}$

$$R(\omega) \simeq R_0 \omega^3, \quad R_0 = \frac{(\sigma_e - \sigma_h)^2}{16\pi^2 \rho c^5}, \quad (13)$$

and we obtain the averaged error $\delta = \alpha^2 R_0 \tau_g^{-2}/3$ (taking into account the upper cut-off, the error will be finite even for an infinitely fast gate (see Fig. 4).

Hence, this non-Markovian error increases as the speed of gate increases. This could result in obtaining arbitrarily low error by choosing suitably low speed of gates. However, if our system is also subjected to other type of noise this becomes impossible. Indeed, if we assume that our system undergoes additional amplitude damping with rate γ_M , the total error per gate is

$$\delta = \frac{\gamma_{nM}}{\tau_g^2} + \gamma_M \tau_g, \quad \gamma_{nM} = \frac{1}{3} \alpha^2 R_0, \quad \gamma_M = \frac{1}{\tau_r}, \quad (14)$$

where τ_r is the characteristic time of exponential decay (Markovian error). As a result, the overall error is unavoidable and optimization is needed. The above formulas lead to

$$\delta_{\min} = \frac{3}{2} (2\gamma_M^2 \gamma_{nM})^{1/3} = \frac{3}{2} \left(\frac{2\alpha^2 R_0}{3\tau_r^2} \right)^{1/3} = \alpha^{2/3} 0.0035,$$

for

$$\tau_g = \left(2 \frac{\gamma_{nM}}{\gamma_M} \right)^{1/3} = \left(\frac{2}{3} \alpha^2 R_0 \tau_r \right)^{1/3} = \alpha^{2/3} 1.5 \text{ ps},$$

where we have used GaAs material parameters (Table 1).

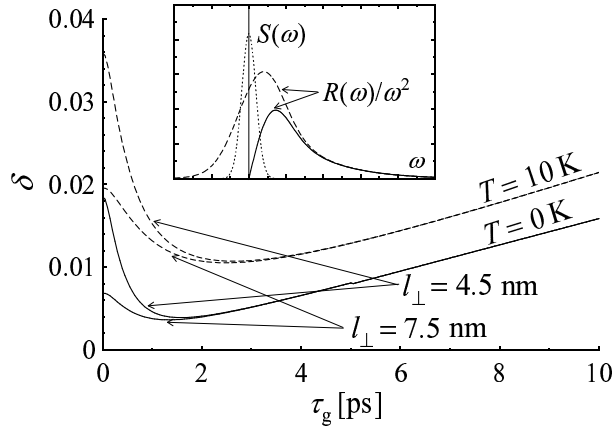


Figure 4. Combined Markovian and non-Markovian error for a $\alpha = \pi/2$ rotation on a qubit implemented as a confined exciton in a InAs/GaAs quantum dot, for $T = 0$ (solid lines) and $T = 10$ K (dashed lines), for two dot sizes (dot height is 20% of its diameter). The Markovian decoherence times are inferred from the experimental data [17]. Inset: Spectral density of the phonon reservoir $R(\omega)$ at these two temperatures and the gate profile $S(\omega)$ for $\alpha = \pi/2$.

The exact solution within the proposed model, taking into account the cut-off and anisotropy of the dot shape and allowing finite temperatures, is shown in Fig. 4. The size-dependent cut-off is reflected by a shift of the optimal parameters for the two dot sizes: larger dots admit faster gates and lead to lower error. Interestingly, the trade-off becomes more apparent at nonzero temperature.

It should be noted that these optimal times are longer than the limits imposed by level separation [39–43]. Thus, the non-Markovian reservoir effects (dressing) seem to be the essential limitation to the gate speed.

5. Conclusions

We have shown that an action performed on the carrier system (e.g. exciton) confined in a quantum dot must be accompanied by an appropriate reconstruction of the lattice state. Such a dressing process takes place spontaneously if the charge distribution is changed on times short compared to timescales of the lattice dynamics (phonon oscillation periods). This spontaneous process destroys the quantum coherence of the system and may preclude quantum information processing or coherent nanotechnology applications.

On the other hand, sufficiently adiabatic operation would take long time compared to the exciton lifetime and other exponential decay processes, again leading to large coherence loss. Therefore, optimal operating conditions for maximum preservation of coherence must be searched for.

We have evaluated the minimal error for typical parameters, showing that the optimal gating time (~ 1 ps) lies within the current experimental possibility. This optimal time sets up the limit beyond which further gate speed-up is unfavorable. It is remarkable that minimal error δ we found ($0.004 - 0.01$), although not extremely high, is still of 1-2 orders of magnitude higher than the one admitted by fault-tolerant schemes known so far ($\sim 10^{-5}$). However, possible improvements of the latter schemes cannot be excluded.

Acknowledgments

This work was supported by the Polish KBN under Grants No. 2 P03B 024 24 and No. 2 P03B 085 25.

References

- [1] S. Hameau, Y. Guldner, O. Verzelen, R. Ferreira, and G. Bastard. Strong electron-phonon coupling regime in quantum dots: evidence for everlasting resonant polarons. *Phys. Rev. Lett.*, 83:4152, 1999.
- [2] S. Hameau, J. M. Isaia, Y. Guldner, E. Deleporte, O. Verzelen, R. Ferreira, G. Bastard, J. Zeman, and J. M. Gérard. Far-infrared magnetospectroscopy of polaron states in self-assembled InAs/GaAs quantum dots. *Phys. Rev. B*, 65:085316, 2002.
- [3] O. Verzelen, R. Ferreira, and G. Bastard. Excitonic polarons in semiconductor quantum dots. *Phys. Rev. Lett.*, 88:146803, 2002.
- [4] L. Jacak, J. Krasnyj, D. Jacak, and P. Machnikowski. Magneto-polaron in a weakly elliptical InAs/GaAs quantum dot. *Phys. Rev. B*, 67:035303, 2003.
- [5] R. Heitz, M. Veit, N. N. Ledentsov, A. Hoffmann, D. Bimberg, P. S. Kop'ev, and Zh. I. Alferov. Energy relaxation by multiphonon processes in InAs/GaAs quantum dots. *Phys. Rev. B*, 56:10435, 1997.
- [6] R. Heitz, H. Born, F. Guffarth, O. Stier, A. Schliwa, A. Hoffmann, and D. Bimberg. Existence of a phonon bottleneck for excitons in quantum dots. *Phys. Rev. B*, 64:241305, 2001.
- [7] Ivan V. Ignatiev, Igor E. Kozin, Valentin G. Davydov, Selvakumar V. Nair, Jeong-Sik Lee, Hong-Wen Ren, Shigeo Sugou, and Yasuaki Masumoto. Phonon resonances in photoluminescence spectra of self-assembled quantum dots in an electric field. *Phys. Rev. B*, 63:075316, 2001.
- [8] O. Verzelen, R. Ferreira, and G. Bastard. Polaron lifetime and energy relaxation in semiconductor quantum dots. *Phys. Rev. B*, 62:R4809, 2000.
- [9] L. Jacak, J. Krasnyj, D. Jacak, and P. Machnikowski. Anharmonicity induced polaron relaxation in InAs/GaAs quantum dots. *Phys. Rev. B*, 65:113305, 2002.
- [10] O. Verzelen, G. Bastard, and R. Ferreira. Energy relaxation in quantum dots. *Phys. Rev. B*, 65:081308, 2002.
- [11] R. Heitz, I. Mukhametzhanov, O. Stier, A. Madhukar, and D. Bimberg. Enhanced polar exciton-lo-phonon interaction in quantum dots. *Phys. Rev. Lett.*, 83:4654, 1999.

- [12] R. Heitz, I. Mukhametzhanov, O. Stier, A. Madhukar, and D. Bimberg. Phonon-assisted polar exciton transitions in self-organized InAs/GaAs quantum dots. *Physica E*, 7:398, 2000.
- [13] A. Lemaître, A. D. Ashmore, J. J. Finley, D. J. Mowbray, M. S. Skolnick, M. Hopkinson, and T. F. Krauss. Enhanced phonon-assisted absorption in single InAs/GaAs quantum dots. *Phys. Rev. B*, 63:161309, 2001.
- [14] F. Findeis, A. Zrenner, G. Böhm, and G. Abstreiter. Phonon-assisted biexciton generation in a single quantum dot. *Phys. Rev. B*, 61:R10579, 2000.
- [15] V. M. Fomin, V. N. Gladilin, S. N. Klimin, and J. T. Devreese. Enhanced phonon-assisted photoluminescence in InAs/GaAs parallelepiped quantum dots. *Phys. Rev. B*, 61:R2436, 2000.
- [16] L. Jacak, J. Krasnyj, and W. Jacak. Renormalization of the Fröhlich constant for electrons in a quantum dot. *Phys. Lett. A*, 304:168, 2002.
- [17] P. Borri, W. Langbein, S. Schneider, U. Woggon, R. L. Sellin, D. Ouyang, and D. Bimberg. Ultralong dephasing time in InGaAs quantum dots. *Phys. Rev. Lett.*, 87:157401, 2001.
- [18] P. Borri, W. Langbein, S. Schneider, U. Woggon, R. L. Sellin, D. Ouyang, and D. Bimberg. Rabi oscillations in the excitonic ground-state transition of InGaAs quantum dots. *Phys. Rev. B*, 66:081306, 2002.
- [19] B. Krummheuer, V. M. Axt, and T. Kuhn. Theory of pure dephasing and the resulting absorption line shape in semiconductor quantum dots. *Phys. Rev. B*, 65:195313, 2002.
- [20] A. Vagov, V. M. Axt, and T. Kuhn. Electron-phonon dynamics in optically excited quantum dots: Exact solution for multiple ultrashort laser pulses. *Phys. Rev. B*, 66:165312, 2002.
- [21] A. Vagov, V. M. Axt, and T. Kuhn. Impact of pure dephasing on the nonlinear optical response of single quantum dots and dot ensembles. *Phys. Rev. B*, 67:115338, 2003.
- [22] L. Jacak, P. Machnikowski, J. Krasnyj, and P. Zoller. Coherent and incoherent phonon processes in artificial atoms. *Eur. Phys. J. D*, 22:319, 2003.
- [23] Robert Alicki, Michał Horodecki, Paweł Horodecki, Ryszard Horodecki, Lucjan Jacak, and Paweł Machnikowski. Optimal strategy of quantum computing and trade-off between opposite types of decoherence. quant-ph/0302058, 2003.
- [24] P. Machnikowski and L. Jacak. Limitation to coherent control in quantum dots due to lattice dynamics. cond-mat/0305165, 2002.
- [25] Gerald D. Mahan. *Many-Particle Physics*. Kluwer, New York, 2000.
- [26] Ulrich Hohenester, Rosa Di Felice, and Elisa Molinari. Optical spectra of nitride quantum dots: Quantum confinement and electron-hole coupling. *Appl. Phys. Lett.*, 75:3449, 1999.

- [27] U. Hohenester, Rosa Di Felice, Elisa Molinari, and Fausto Rossi. Theoretical analysis of the optical spectra of $\text{In}_x\text{Ga}_{1-x}\text{N}$ quantum dots in $\text{In}_y\text{Ga}_{1-y}\text{N}$ layers. *Physica E*, 7:934, 2000.
- [28] S. De Rinaldis, I. D’Amico, E. Biolatti, R. Rinaldi, R. Cingolani, and F. Rossi. Intrinsic exciton-exciton coupling in gan-based antum dots: Application to solid-state quantum computing. *Phys. Rev. B*, 65:081309, 2002.
- [29] Sadao Adachi. GaAs, AlAs and AlGaAs: Material parameters for use in research and device applications. *J. Appl. Phys.*, 58:R1, 1985.
- [30] D. Strauch and B. Dorner. Phonon dispersion in GaAs. *J. Phys: Cond. Matt.*, 2:1457, 1990.
- [31] Andris Suna. Green’s function approach to exciton–phonon interaction. *Phys. Rep.*, 135:A111, 1964.
- [32] A. A. Abrikosov, L. P. Gorkov, and I. E. Dzyaloshinski. *Methods of Quantum Field Theory in Statistical Physics*. Dover Publications, New York, 1975.
- [33] V. L. Bonch-Bruевич and S. V. Tyablikov. *The Green Function Method in Statistical Mechanics*. North-Holland, Amsterdam, 1962.
- [34] A. C. Davydov and G. M. Pestryakov. On the canonical transformation in the theory of exciton-phonon interaction. *Phys. Stat. Sol. (b)*, 49:505, 1972.
- [35] M. Bayer and A. Forchel. Temperature dependence of the homogeneous linewidth in $\text{In}_{0.60}\text{Ga}_{0.40}\text{As}/\text{GaAs}$ self-assembled quantum dots. *Phys. Rev. B*, 65:041308, 2002.
- [36] F. Vallée and F. Bogani. Coherent time-resolved investigation of LO-phonon dynamics in GaAs. *Phys. Rev. B*, 43:12049, 1991.
- [37] F. Vallée. Time-resolved investigation of coherent LO-phonon relaxation in III-V semiconductors. *Phys. Rev. B*, 49:2460, 1994.
- [38] Robert Alicki, Michal Horodecki, Pawel Horodecki, and Ryszard Horodecki. Dynamical description of quantum computing: generic nonlocality of quantum noise. *Phys. Rev. A*, 65:062101, 2002. quant-ph/0105115.
- [39] E. Biolatti, R. C. Iotti, P. Zanardi, and F. Rossi. Quantum information processing with semiconductor macroatoms. *Phys. Rev. Lett.*, 85:5647, 2000.
- [40] Pochung Chen, C. Piermarocchi, and L. J. Sham. Control of exciton dynamics in nanodots for quantum operations. *Phys. Rev. Lett.*, 87:067401, 2001.
- [41] C. Piermarocchi, Pochung Chen, Y .S. Dale, and L. J. Sham. Theory of fast quantum control of exciton dynamics in semiconductor quantum dots. *Phys. Rev. B*, 65:075307, 2002.
- [42] Lin Tian and Seth Lloyd. Resonant cancellation of off-resonant effects in a multilevel qubit. *Phys. Rev. A*, 62:050301, 2000.
- [43] L.-A. Wu, M. S. Byrd, and D. A. Lidar. Efficient universal leakage elimination for physical and encoded qubits. *Phys. Rev. Lett.*, 89:127901, 2002.